Received: 1 April 2021 | Revised: 11 August 2021 | Accepted: 14 September 2021

DOI: 10.1002/aic.17498

REACTION ENGINEERING, KINETICS AND CATALYSIS

AIChE JOURNAL

High-yield production of *p*-diethynylbenzene through consecutive bromination/dehydrobromination in a microreactor system

Zhirong Yang | Yue Yang | Xuefeng Zhang | Wei Du | Jing Zhang | Gang Qian | Xuezhi Duan | Xinggui Zhou

State Key Laboratory of Chemical Engineering, East China University of Science and Technology, Shanghai, China

Correspondence
Jing Zhang, State Key Laboratory of Chemical Engineering, East China University of Science and Technology, Shanghai 200237, China.
Email: jingzhang8507@ecust.edu.cn

Xinggui Zhou, State Key Laboratory of Chemical Engineering, East China University of Science and Technology, Shanghai 200237, China.
Email: xgzhou@ecust.edu.cn

Funding information
China Postdoctoral Science Foundation, Grant/Award Numbers: 2019TQ0093, 2020M671025; Natural Science Foundation of Shanghai, Grant/Award Number: 20ZR1415700; National Natural Science Foundation of China, Grant/Award Numbers: 21991103, 21991104, 22008072, 22008074

Abstract

Polyarylacetylene resins have received great attention due to their outstanding heat resistance, while the absence of an efficient method to produce their monomer, *p*-diethynylbenzene (*p*-DEB), has discouraged their commercial development. Industrial production of *p*-DEB consists of bromination and dehydrobromination in a semi-batch reactor, state of the art yield from which is only 70%–75%. Herein, a combined effort of byproduct characterization and density functional theory calculations revealed that side reactions mainly consisted of aromatic substitution which would be promoted by thermal runaway derived from exothermic bromination due to higher activation energy of side reactions. From these considerations, we developed a microreactor system to enhance heat transfer thereby mitigating byproduct formation, from which a *p*-DEB yield of 99.2% could be achieved. Moreover, the high heat removal efficiency avoided the use of slow feeding and reactant dilution required in semi-batch operation, thereby shortening the reaction time to 14 s while generating more concentrated product.

KEYWORDS
bromination, heat transfer, microreactor, *p*-diethynylbenzene, process intensification

1 | INTRODUCTION

Polyarylacetylene (PAA) resins have been the subject of extensive research due to their outstanding heat resistance and excellent process properties.[1,2] One major drawback of traditional high temperature resins, for example, phenolic resins, is the evolution of volatiles, such as water or ammonia, that cause void formation during processing, limiting their utilization in many applications.[3,4] In contrast, PAA resins can be shaped without gas evolution since their thermal cure is through addition reactions rather than condensation reactions, making PAA suitable to many important low pressure process techniques. Moreover, PAA resins have good electrical and optical properties, such as high conductivity, high charge/weight storage capability, and large third-order nonlinear optical susceptibility.[5] Therefore, PAA resins have been regarded as the next generation ablative materials favorable in aerospace/military field and potentially useful new materials of optoelectronic devices for applications in solar-to-fuel energy conversions.[6–15] However, their full commercial development has been discouraged by the absence of an efficient and safe method to produce the PAA monomer, *p*-diethynylbenzene (*p*-DEB).[16]

Three syntheses routes: aromatics acylation,[17,18] trimethylsilylacetylene method,[19] and halogenation/dehydrohalogenationof divinylbenzene[1,20] have been developed to produce *p*-DEB. However, the first two methods have not been used industrially due to their operational complexities, expensive reagents, difficulty and high risk in separation/purification, and so forth. The third route was first reported by Allan S. Hay in 1960 and has become the dominant method for industrial production of *p*-DEB

(e.g., Hercules Incorporated, General Electric Company, etc.), which consists of bromine addition of *p*-divinylbenzene (*p*-DVB) and consecutive dehydrobromination in alkaline solution (Scheme 1).[1,21] However, severe challenges in reaction temperature control and separation significantly affect the production efficiency of *p*-DEB. The reactant, DVB, is produced through dehydrogenation of diethylbenzene, which results in a mixture containing *m*-DVB, *p*-DVB, *m*-ethyl-vinylbenzene (*m*-EVB), and *p*-EVB. These four chemicals are difficult to separate due to their similar boiling points. Owing to the absence of high purity *p*-DVB, the isomer containing *p*-DEB product needs to undergo rigorous separation. Instead, purification of the reactant (*p*-DVB) prior to reaction seems more economical; however, the method for doing so is currently lacking. More importantly, the exothermic bromination was proposed to favor side reactions, although limited work has been reported to unravel their pathways. It was reported that the temperature should be limited in the range of 10–15°C during the bromination in a batch reactor, which requires slow feeding rate of bromine and diluted reactants.[1,20] Even with careful control of the feeding rates and concentrations, state of the art yield of the *p*-DEB can only reach 70%–75%.[1,20] In this regard, design and fabrication of a reactor system capable of efficient heat removal thereby avoiding side reactions, shortening feeding/reaction time, and improving product concentration is highly desirable.

To address the above issues, we explored a π-complexation method[22–25] using CuCl to purify the *p*-DVB from its commercial crude which contains large amounts of isomers and impurities. The relationship between complexation/decomplexation temperature and separation efficiency has been built, based on which a *p*-DVB purity higher than 99% was achieved after two consecutive complexation/decomplexation and was used as the reactant thereafter. Then, we studied the effect of temperature on the yield of target product in a batch reactor and identified chemical structures of byproducts. Subsequent density functional theory (DFT) calculations revealed that the side reactions mainly consisted of aromatic substitution and the thermal runaway would favor the side reaction due to its much higher activation energy compared to that of target reaction. From these considerations, we developed and fabricated a microreactor system to intensify heat transfer thereby mitigating the thermal runaway derived byproduct formation. According to heat and mass transfer evaluation, efficient mixing and heat removal can be achieved by tuning reactor size and flow rate, after which the influence of operating conditions on the conversion and yield was systematically investigated. As a result, an unprecedented *p*-DEB yield of 99.2% could be achieved within only a few seconds under optimized conditions through continuous synthesis in the two-stage microreactor system consisting of bromination and dehydrobromination. Moreover, the microreactor system overcame the restrictions of feeding rates and reactant concentrations associated with semi-batch operation, allowing more concentrated product to be obtained. To the best of our knowledge, this work demonstrates, for the first time, the use of a microreactor system for rapid and high-yield production of *p*-DEB, which reveals a new avenue to boost commercial development of its polymer, PAA resins.

2 | EXPERIMENTAL

2.1 | Purification of *p*-DVB

Commercial DVB mainly contains four compounds, *m*-DVB (50.6 wt%), *p*-DVB (29.7 wt%), *m*-EVB (11.9 wt%), and *p*-EVB (7.8 wt%). In the current study, π-complexation method was used to obtain high purity *p*-DVB from its commercial crude. In a typical experiment, 6.8 g CuCl powder was ultrasonically dispersed in 50 ml 2 wt% methanol/toluene solution. Then, 10 g crude DVB was added into the solution to react with the CuCl for 0.75–3 h at a temperature range of 10–35°C. The yellow complex compound was filtered and washed twice with toluene, after which the complex compound was mixed with toluene with a 1:5 ratios by volume at 60–95°C and filtered once the decomplexation was completed. The *p*-DVB rich filtrate was then concentrated using a rotary evaporator. The chemical composition of the filtrate was analyzed by a gas chromatograph (GC; 4890D; Agilent Technologies) equipped with a mass spectrometer (MS) using a HP-5 capillary column. For temperature ramping program, the initial temperature of the GC oven was held at 40°C for 3 min. Then, the temperature was ramped to 250°C with a rate of 5°C/min, after which the temperature was held at 250°C for 10 min.

2.2 | Synthesis of *p*-DEB in a semi-batch reactor

For bromination, a certain amount of Br_2/CCl_4 solution (20–50 wt%, 5–15 ml) was added dropwise with a feeding rate of 0.1–2.5 ml/min into the *p*-DVB/toluene solution (10–60 wt%, 10–20 ml) in a 100 ml volume three-necked flask with a water jacket at a temperature range of 5–25°C. During the feeding and reaction, the stirring rate was kept at 600 rpm. Heat transfer fluid flowed around the external jacket of the reactor for temperature control. After a certain time, the reaction

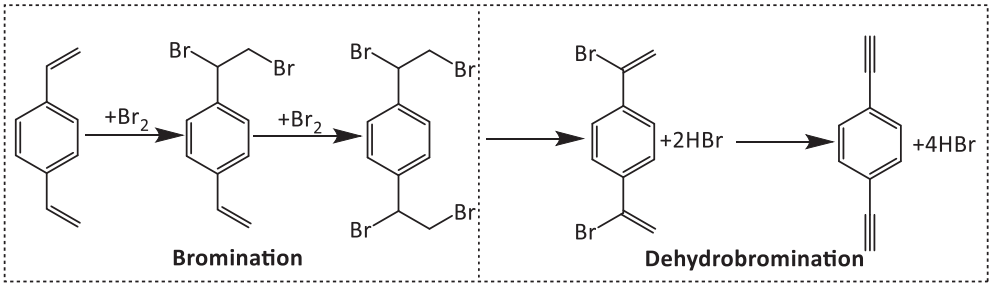

SCHEME 1 Synthesis route of *p*-DEB from bromination of *p*-DVB followed by dehydrobromination. *p*-DEB, *p*-diethynylbenzene; *p*-DVB, *p*-divinylbenzene

was terminated by adding proper amount of NaOH/ethanol(EtOH) to consume the residue Br_2. The postreaction solution after the bromination was filtrated and concentrated to (partially) remove precipitates and toluene solvent. Then, a certain amount of preheated 30 wt% NaOH/EtOH solution was added to the 1,4-bis(1,2-dibromoethyl) benzene (*p*-DVB-Br_4) solution to accelerate the dehydrobromination. The dehydrobromination was performed at a temperature range of 70–95°C, during which a reflux condenser was used to capture the volatiles. The product analysis was performed using the GC-MS system as mentioned previously. In the current study, all yields refer to the GC yield which was calculated by external standard method.

2.3 | Synthesis of *p*-DEB in a microreactor system

A two-stage microreactor system was used in the current study for continuous production of *p*-DEB through bromination and dehydrobromination.[26] Figure 1A shows the configuration of the microreactor system. The two micro T-mixers and all coils were completely immersed in a waterbath. The micro T-mixer has two identical opposed inlet channels of 0.3-mm wide and 0.1-mm deep, the outlet channel of which is 0.3 mm in diameter (Figure 1B). All coils have an inner diameter of 1 mm and the lengths of the preheat coils were determined by heat transfer calculation. First, the DVB/toluene solution was brought into contact with Br_2/CCl_4 solution in the micro T-mixer, the effluent of which was then mixed with 30 wt% NaOH/EtOH solution in the second micro T-mixer. The reaction temperatures of bromination and dehydrobromination were in the range of 10–50°C and 70–90°C, respectively. Titanium coils were used to transfer Br_2 containing fluid due to their high corrosion resistance. For the dehydrobromination process, copper coils were used due to their high thermal conductivity and lower cost. The product analysis was performed using the GC-MS system as mentioned previously.

2.4 | DFT calculations

The activation energy E_a and reaction enthalpy *H* of bromine addition and side reaction (aromatic substitution) were estimated by Gaussian 09 (Revision D.01). Geometry optimizations were performed at DFT/wb97xd level with the 6-31G* (d, p) basis set. Frequency analysis was conducted at the same level of theory to verify the stationary points to be minima (no imaginary frequencies) or transition states (only one imaginary frequency). The relative energies with ZPE corrections and free energies are in kJ/mol. The single-point energies were computed with M062X/def2tzvp basis sets. Conductor-like polarizable continuum model for toluene was used in both geometry optimizations and computation of single-point energies.[27] In addition, the π-complexation binding energy was calculated using Gaussian 09 (Revision D.01) software, during which the geometry optimization and bond energy analysis were performed at DFT/B3LYP level with the 6-311G** basis set and menthol–toluene as solvent.[22–25]

3 | RESULTS AND DISCUSSION

3.1 | Purification of *p*-DVB

Table 1 shows the results of *p*-DVB purification through complexation and decomplexation at different temperatures. The *p*-DVB content among total DVB in the precipitate after the complexation is about 89% at temperatures of 10–20°C. Further increasing the complexation temperature shortened the equilibrium time at the expense of separation efficiency. Therefore, 18–20°C is the optimal complexation temperature when the measured complex equilibrium constant for *p*-DVB is two orders of magnitude higher than the one for *m*-DVB, which is consistent with the stronger complexation binding energy of the former than that of the latter (Figure S1). During the decomplexation, higher temperature is conducive to decomplexation but tends to trigger self-polymerization of DVB. In this regard, the optimal decomplexation temperature is 80°C under which a total DVB yield of 95.5% was achieved. In general, thorough separation of *p*-DVB from *m*-DVB needs twice complexation/decomplexation. As shown in Scheme 2, 89.0% *p*-DVB was obtained after the first complexation/decomplexation without consideration of solvents, while the value went up to 99.6% after the second complexation/decomplexation.

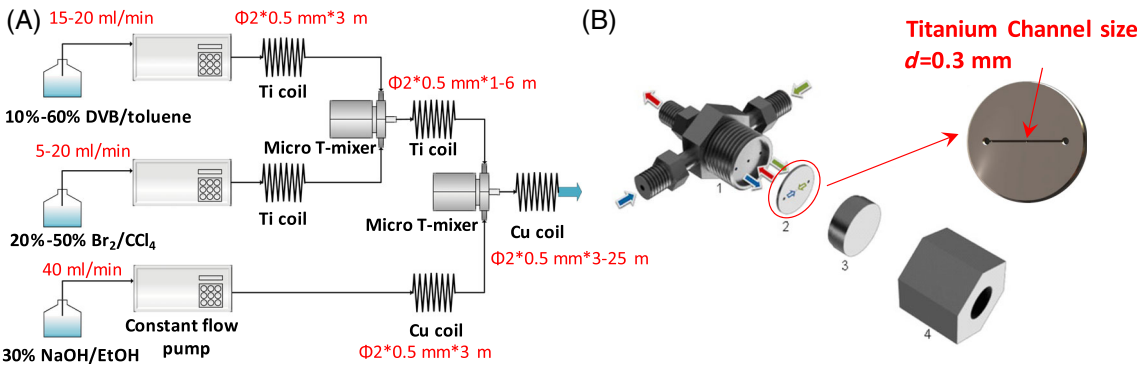

FIGURE 1 (A) Continuous synthesis of *p*-DEB in the microreactor system. (B) Configuration of the T-mixer with inlet/outlet (1), mixing plate (2), cover plate (3), and fixing bolt (4). *p*-DEB, *p*-diethynylbenzene

TABLE 1 Effect of temperature on separation efficiency through complexation and decomplexation

Complexation[a]					Decomplexation[a]	
Temperature (°C)	Equilibrium time (min)	*p*-DVB yield (%)[b]	*p*-DVB (%)[c]	*m*-DVB (%)[c]	Temperature (°C)	*p*-DVB yield (%)[d]
10	180	91.2	89.0	11.0	65	32.5
15	150	91.1	88.9	11.1	70	69.4
18	75	90.5	89.1	10.9	75	85.7
20	60	90.3	89.0	11.0	80	95.5
22	60	79.5	87.6	12.4	85	90.4
25	45	75.3	83.3	16.7	90	89.8
30	45	70.2	80.2	19.8	95	80.2

Abbreviations: *p*-DVB, *p*-divinylbenzene; GC, gas chromatograph.
[a]All yields refer to GC yield.
[b]Amount of *p*-DVB in the precipitate after complexation divided by amount of *p*-DVB prior to complexation.
[c]Amount of DVB isomers in the precipitate divided by total amount of DVB in the precipitate.
[d]Amount of *p*-DVB in the decomplexation solution divided by amount of *p*-DVB prior to the decomplexation.

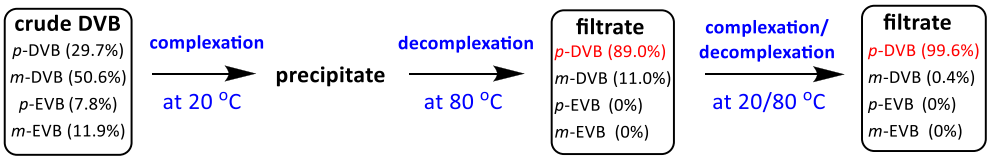

SCHEME 2 Purification of *p*-DVB from commercial DVB crude through complexation and decomplexation. *p*-DVB, *p*-divinylbenzene

3.2 | Bromination of *p*-DVB in a semi-batch reactor

Figure 2A shows almost complete conversion of *p*-DVB over a temperature range of 5–25°C, among which the highest yield (70.1%) of target product, *p*-DVB-Br_4, was achieved at 10°C. It is important to note that the abovementioned temperature only refers to waterbath temperature. The byproducts are in the form of white precipitate. Effects of reactant feeding rate and concentration were also investigated. Figure 2B–D shows the *p*-DVB-Br_4 yield decreased with increasing Br-feeding rate and reactant concentrations. These results are consistent with literature that the bromination temperature should be controlled between 10–15°C and low feeding rate and reactant concentration are desired to maximize the yield of *p*-DVB-Br_4.[1,20,21] Since thermal runaway derived from the exothermic bromine addition was reported as the cause for side reactions,[1,21] time on stream reaction temperature was recorded at different water-batch temperatures and feeding rates. As shown in Figure 2E,F, severe thermal runaway (15–20°C) was observed even at a Br_2 feeding rate as low as 0.5 ml/min, and the degree of thermal runaway increased with the feeding rate accompanied by lower yield of *p*-DVB-Br_4. In the current batch operation, the *p*-DVB-Br_4 yield can reach up to 85.0% within 10°C water-batch using very low reactant concentrations (C_{Br} = 10 wt%, C_{DVB} = 20 wt%) and Br_2 feeding rate (1 ml/min), where the reaction rates were limited by the feeding rates and the use of diluted reactants would raise energy consumption in downstream separation.

Surprisingly, chemical structures of the byproducts from *p*-DVB bromination have been seldomly reported, possibly due to a lack of mass spectra information of brominated aromatic compounds in NIST database. However, byproduct identification is important to unravel reaction pathways and guide the design of reaction system. In the current study, byproduct characterization was performed by dissolving the precipitated byproducts from the semi-batch *p*-DVB bromination, the solution of which then underwent GC-MS analysis. The results were shown in Figure 3 where the five major peaks were identified through molecular ion analysis utilizing the unique isotopic pattern of bromine: the abundances of ^{79}Br and ^{81}Br are 51% and 49%, respectively. For Peak 1, an approximately 1:1 ratio of molecular ion 208–210 (Figure S2[1]) suggests a chemical structure of 2-bromo-1,-4-divinylbenzene. Moreover, an approximately 1:2:1 ratio of molecular ion 286:288:290 and an approximately 1:1 ratio of *m*/*z* 207:209 (Figure S2[3–5]) suggest Peak 3–5 being three isomers of dibromo-*p*-divinylbenzene. Similarly, an approximately 1:2:1 ratio of molecular ion 288:290:292 and an approximately 1:1 ratio of *m*/*z* 209:211 (Figure S2[2]) suggest Peak 2 being 1-(1,2-dibromoethyl)-4-vinylbenzene, the presence of which may be caused by insufficient Br_2 for complete bromine addition due to Br_2 evaporation during feeding. The characterization results revealed that side reactions during the bromination of *p*-DVB mainly consist of aromatic substitution with bromine.

The Gibbs free energy of each state involved in bromine addition and aromatic substitution was obtained using DFT calculations, as illustrated in Figure 4. The optimized geometries of each state are shown in Figure S3. The computational results reveal that the second aromatic substitution with bromine to produce a bromine substituted intermediates (TS-2) is the rate-limiting step for aromatic substitution, while the second bromine addition to produce a bromide intermediate

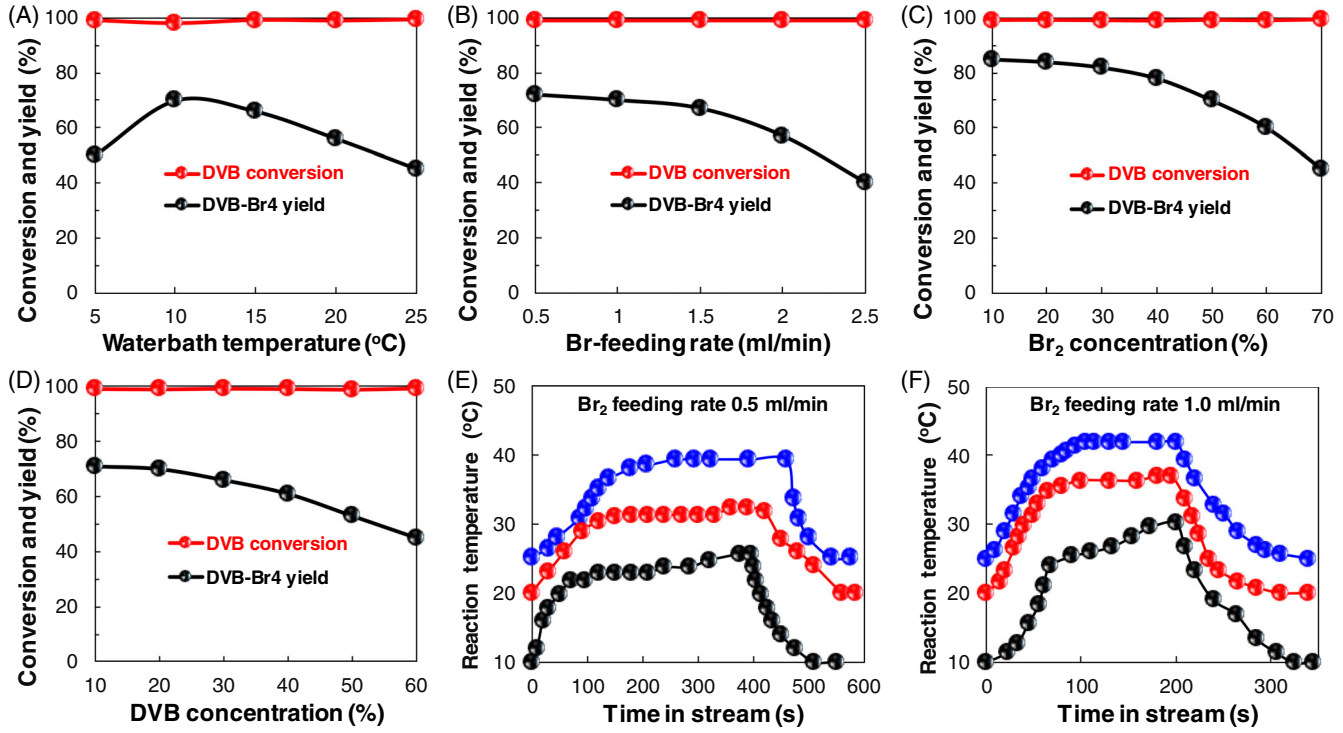

FIGURE 2 Effects of (A) temperature, (B) Br-feeding rate, Fd_{Br}, (C) Br_2 concentration, C_{Br}, and (D) *p*-DVB concentration, C_{DVB}, on *p*-DVB bromination in a semi-batch reactor. (E and F) Time on stream reaction temperature under different Br-feeding rate at waterbath temperatures of 10°C, 20°C and 25°C. Conditions: (A) Fd_{Br} = 1 ml/min, C_{Br} = 50 wt%, C_{DVB} = 20 wt%; (B) T = 10°C, C_{Br} = 50 wt%, C_{DVB} = 20 wt%; (C) Fd_{Br} = 1 ml/min, T = 10°C, C_{DVB} = 20 wt%; (D) Fd_{Br} = 1 ml/min, T = 10°C, C_{Br} = 50 wt%; (E and F) C_{Br} = 50 wt%, C_{DVB} = 20 wt%. For all experiments, the Br_2/C═C bond mole ratio was controlled at 1.02. Analysis was performed at 15 min after dropwise feeding of Br_2 to ensure complete bromination. *p*-DVB, *p*-divinylbenzene

FIGURE 3 Characterization of byproducts using GC-MS. Mass spectrometer ion fragmentations of Peaks 1–5 were listed in Figure S2. GC-MS, gas chromatograph–mass spectrometer

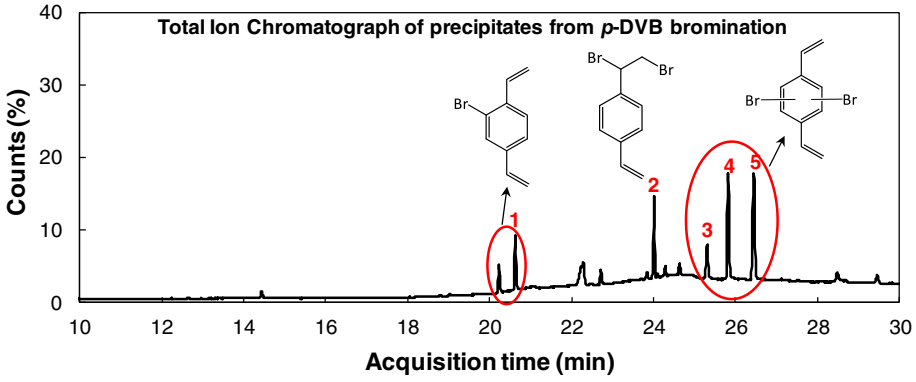

(TS-2) is the rate-limiting step for bromine addition. Figure 4 shows that the calculated activation energy (E_a) for aromatic substitution is 244.8 kJ/mol, which is much higher than the E_a of bromine addition (59.9 kJ/mol). Therefore, the DFT calculations suggest that an increase of reaction temperature would promote aromatic substitution to a much higher degree than bromine addition, which unravels the relationship between thermal runaway and side reactions. The reaction enthalpy of bromine addition and aromatic substitution were also obtained using DFT calculations (Figure S4), which was used for heat transfer calculations to estimate the degree of thermal runaway during synthesis of *p*-DVB-Br_4 in the following microreactor system.

According to the above analysis, microreaction technology should be a desired strategy to mitigate the side reactions caused by thermal runaway, due to the excellent heat transfer efficiency derived from high surface area to volume ratio of the microreactor. The ΔH_m for bromine addition of *p*-DVB is −202.4 kJ/mol, according to DFT calculations (Figure S4). The heat removal capacity of the microreactor was estimated using heat transfer calculations.[31] The wall temperature of the microreactor was assumed to be constant and equal to the water bath temperature since the heat transfer resistance of the tube wall is negligible compared to that inside the tube. In typical reaction conditions, the heat production rate of complete bromine addition within

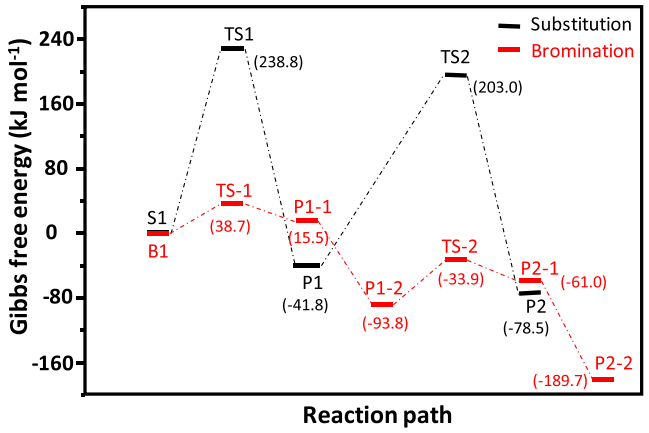

FIGURE 4 Relative Gibbs free energy (kJ/mol) of each state involved in bromine addition of *p*-DVB to produce *p*-DVB-Br_4 (target product) and aromatic substitution of *p*-DVB to produce 1,4-dibromo-2,5-divinylbenzene (byproduct). The activation energy was determined by energy difference of rate-limiting step.[28–30] *p*-DVB, *p*-divinylbenzene

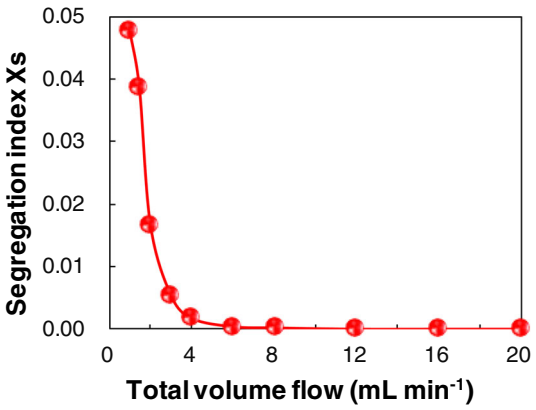

FIGURE 5 Effect of total flow rate on *Xs*

the microreactor is $Q_{prod} = q_v C_0(-\Delta H_m) = 40 \times 10^{-3} \times 0.6676 \times 202.4$ kJ/min = 90.1 J/s, where the total flow rate q_v is 40 ml/min and the tube length is 4 m. Then, the Reynolds number was calculated as follows, $Re = du\rho/\mu = 10^{-3} \times 0.8488 \times 1312/0.000787 = 1415$, suggesting a turbulence flow profile given an early transition from laminar to turbulent flow in microreactor system.[32–34] Thus, the heat transfer coefficient can be calculated as $\alpha = 0.023(\lambda/d)Re^{0.8}(Cp\mu/\lambda)^{0.3} = 1538$W m^{-2} K^{-1},where the average thermal conductivity of the solvent λ is 0.1121 W m^{-1} K^{-1} and the heat capacity C_p is 1109 J kg^{-1} K^{-1}. So, the required logarithmic mean temperature differences of the fluid flow (ΔT_m) to equate heat production rate with heat removal rate ($Q_{prod} = Q_{rem} = \alpha A \Delta T_m$) is 4.6°C, suggesting a much lower degree of thermal runaway compared to that of batch reactor shown in Figure 2E,F.

3.3 | Bromination of *p*-DVB in microreactor

Mixing efficiency of the T-mixer microreactor was evaluated using the Villermaux/Dushman reaction which is known to characterize homogeneous mixing. The mixing quality was described under various total liquid flow rates using segregation index (*Xs*). The smaller *Xs* suggests better mixing performance. The details of which calculation process were listed in the Supporting information.[26,35,36] Figure 5 shows the value of *Xs* reduce to zero when the total flow rate is higher than 8 ml/min, suggesting the mixing is rapid and almost instantaneous in this flow range. In the following studies, the total flow rates were kept well above 8 ml/min to ensure a good mixing performance.[37]

Then, the influence of operating conditions on the bromination of *p*-DVB in microreactor system was investigated. As shown in Figure S5, a slight overdose (2%) of Br_2 is desired to promote the bromination, possibly due to inhibition of HBr removal from the *p*-DVB-Br_4. However, excessive amount of Br_2 would negatively affect the subsequent dehydrobromination due to formation of NaBrO to produce disodium terephthalate byproduct by reacting with 1,4-bis (1-bromovinyl) benzene. Furthermore, the effects of temperature and channel size were investigated in a microreactor system with T-mixer size of 0.3 mm and outlet coil of 1 mm in diameter. The yield of *p*-DVB-Br_4 reached 99% at 25°C (Figure 6A, red line). Further increasing temperature lowered the *p*-DVB-Br_4 yield accompanied by appearance of white precipitates due to occurrence of side reactions, which is consistent with batch operations. Even at temperature as low as 10°C, the *p*-DVB-Br_4 yield can reach 99% by slightly prolonging the residence time. In contrast, when the channel size increased to 2 mm for the T-mixer and outlet coil (Figure 6A, black line), the maximum *p*-DVB-Br_4 yield can only reach 70% at 35°C due to severe side reactions as suggested by formation of white precipitates.

We assumed the different reaction performance was mainly due to different heat removal capability as "surface area to volume ratio" of microreactor system changes dramatically with its channel size. In this regard, we estimated the degree of "thermal runaway" by calculating logarithmic mean temperature difference (ΔT_m) of the fluid flow under reaction conditions using the same method as previous section. The detailed calculations are shown in Table S2. The calculated ΔT_m for the narrower microreactor is only approximately 5°C, in contrast to approximately 25°C for its counterpart. Interestingly, the approximately 25°C ΔT_m for reactor with larger channel is similar as the temperature rise in previous semi-batch operations (Figure 2E,F). The results suggest that properly tuning the channel size of microreactor system can mitigate the thermal runaway to an extent that not triggering side reactions during the bromination. Figure S6 shows the yield of *p*-DVB-Br_4 maintained over 99% even at a *p*-DVB concentration of 70%. Therefore, with the intensified heat/mass transfer brought by the microreactor system, the restrictions of reactant concentrations and feeding rates associated with semi-batch operations can be overcome, thereby improving product concentration and lowering energy consumption in separation. Nevertheless, during the continuous production in the microreactor system, a *p*-DVB concentration lower than 60% is suggested to prevent precipitation of *p*-DVB-Br_4. In order to estimate the apparent reaction rate constant and reaction orders of bromine addition, we recorded conversion of

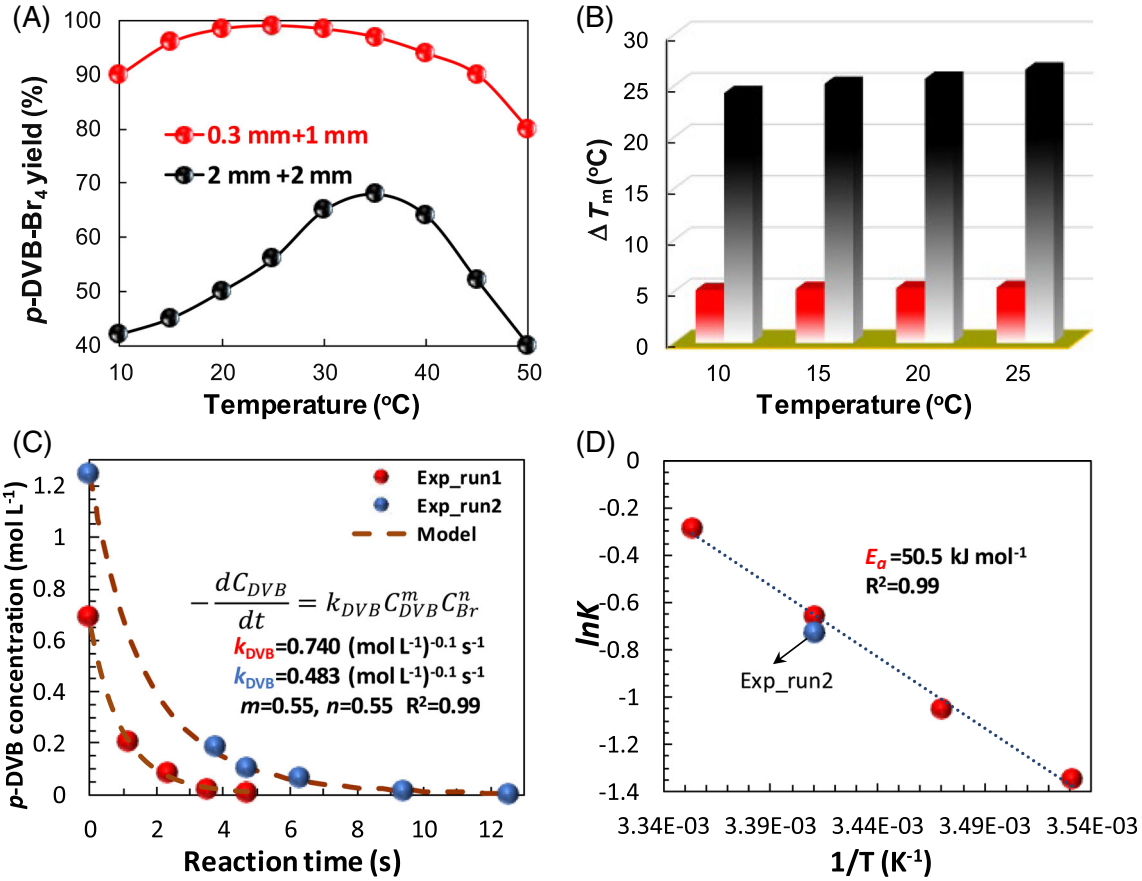

FIGURE 6 (A) Effect of temperature and channel size on product yield, (B) effect of channel size on degree of thermal runaway (represented by ΔT_m), (C) *p*-DVB concentrations at different conditions: experimental (symbols) and kinetic model (dash lines), (D) Arrhenius plot of bromine addition during the bromination of *p*-DVB in microreactor system. Characteristic size of the T-mixers: 2 mm for black line and column in (A) and (B), 0.3 mm for all other cases. Inner diameter of capillary coil at the T-mixer outlet: 2 mm for black line and column in (A) and (B), 1 mm for all other cases. ΔT_m: logarithmic mean temperature difference of the fluid flow. Conditions: (A and B) total flow rate of 20 ml/min, C_{DVB} = 20 wt%, C_{Br} = 50 wt%, residence time = 7 s, Br_2/C=C bond mole ratio = 1.02; (C) Exp_run1: total flow rate = 20 ml/min, C_{DVB} = 20 wt%, C_{Br} = 50 wt%, Br_2/C=C bond mole ratio = 1.02, temperature = 25°C, residence time was changed by tuning the coil length; Exp_run 2: C_{DVB} = 30 wt%, C_{Br} = 50 wt%, Br_2/C=C bond mole ratio = 1.02, temperature = 20°C, coil length = 4 m, residence time was changed by tuning the total flow rates from 50 to 10 ml/min; (D) reaction rate constants at 10–25°C were obtained from product yields in red line (A) and kinetic model in (C). *p*-DVB, *p*-divinylbenzene

p-DVB at different residence times and reactant temperatures in the microreactor system where the thermal runaway could be mitigated to not causing side reactions. The kinetics of bromine addition was established using a power law-type model (Equation 1), which was solved by Runge–Kutta method. The apparent reaction orders and reaction rate constant were determined by fitting the experimental data using a Levenberg–Marquardt algorithm that minimizes the sum of the squared residuals between experimental and fitted concentrations (Figure 6C). The apparent activation energy of bromine addition was then obtained by the Arrhenius equation using reaction rate constants at different temperatures (Figure 6D), the value of which is close to the one from DFT calculations. The representative Matlab® codes are provided in the Supporting information. In summary, the results of microreactor system verified that the precise temperature control is essential to direct reaction pathways during the *p*-DVB bromination. Adjustment of the microreactor channel size plays a key role to ensure high heat removal efficiency, from which high-yield of *p*-DVB-Br_4 was achieved with a reaction residence time of only a few seconds. Here, we demonstrated that the yield of *p*-DVB-Br_4 reach 99% at conditions of total flow rate of 20–40 ml/min, C_{DVB} = 20–50 wt%, C_{Br} = 50 wt%, residence time of more than 7 s, and Br_2/C=C bond mole ratio = 1.02.

$$-\frac{dC_{DVB}}{dt} = k_{DVB}C_{DVB}^{m}C_{Br}^{n} \quad (1)$$

3.4 | Dehydrobromination of *p*-DVB-Br_4 in a batch reactor versus a microreactor

The effect of NaOH usage during the dehydrobromination was investigated (Figure S7), which shows that the maximum *p*-DEB yield was obtained when NaOH/Br mole ratio reached 2.5 for both semi-batch operation and continuous operation in microreactor. The results

TABLE 2 Effect of temperature on dehydrobromination of *p*-DVB in the batch reactor and microreactor

	Batch reactor (yield, %)[a]			Microreactor (yield, %)		
Temperature (°C)	*p*-DVB-Br_4	*p*-DVB-Br_2	*p*-DEB	*p*-DVB-Br_4	*p*-DVB-Br_2	*p*-DEB
75	0	48.2	50.8	24[b]	0[b]	76[b]
85	0	10.3	89.7	3.6[b]	2.2[b]	94.2[b]
90	0	0.8	99.2	0.6[b]/0[c]	1.2/0.5[c]	98.2[b]/99.5[c]

Note: For microreactor, *p*-DVB-Br_4 solution was obtained from continuous bromination at $C_{DVB} = 20$ wt%, $C_{Br} = 50$ wt%, $T = 25°C$, residence time of 4.7 s.

Abbreviations: p-DEB, *p*-diethynylbenzene; *p*-DVB, *p*-divinylbenzene.

[a]Batch reactor: NaOH/Br mole ratio of 2.5, reaction time of 3 h, *p*-DVB-Br_4 reactant was obtained from semi-batch operation at $C_{DVB} = 20$ wt%, $C_{Br} = 50$ wt%, $Fd_{Br} = 1$ ml/min, $T = 10°C$.

[b]Microreactor: T-mixer channel size of 0.3 mm, NaOH/Br mole ratio of 2.5, total flow rate of 79.5 ml/min (1.69 m/s), residence time of 11.8 s (copper coil length = 20 m, 1 mm i.d.).

[c]Microreactor: T-mixer channel size of 0.3 mm, NaOH/Br mole ratio of 2.5, total flow rate of 79.5 ml/min (1.69 m/s), residence time of 14.7 s (copper coil length = 25 m, 1 mm i.d.).

TABLE 3 Composition of postreaction solution and *p*-DEB yield from continuous synthesis of *p*-DEB from *p*-DVB in the two-stage microreactor system

Mass fraction of each component (wt%)							Yield (%)
Ethanol	NaBr	CCl_4	NaOH	Toluene	*p*-DEB	H_2O	*p*-DEB
32.0	21.8	16.8	12.7	6.8	6.6	3.3	99.2%

Note: Bromination condition: $C_{DVB} = 50$ wt%, $C_{Br} = 50$ wt%, Br_2/C=C bond mole ratio = 1.02, $T = 25°C$, residence time = 4.7 s, total flow rate of 39.5 ml/min (0.84 m/s); dehydrobromination condition: $C_{NaOH/EtOH} = 30\%$, NaOH/Br mole ratio = 2.5, $T = 90°C$, residence time = 8.8 s, total flow rate of 79.5 ml/min (1.69 m/s).

Abbreviations: *p*-DEB, *p*-diethynylbenzene; *p*-DVB, *p*-divinylbenzene.

suggest that extra amount of NaOH is beneficial to complete dehydrobromination. Table 2 compares the dehydrobromination behavior in batch reactor and microreactor. In the batch reactor, elimination of the first two moles of HBr to form *p*-DVB-Br_2 easily occurred even at 70°C, but complete dehydrobromination required higher temperature (90°C) and long reaction time (3 h). In contrast, a 98.2% yield of *p*-DEB was achieved within only 12 s of reaction residence time in the microreactor system, although a reaction temperature of 90°C was also required. It should be noted that for both reaction systems, a reaction temperature higher than 90°C would lead to the formation of brown precipitate, possibly due to polymerization of the *p*-DEB. Given the removal of last two moles of HBr to form the *p*-DEB is strongly endothermic,[1] the much shorter reaction time for complete dehydrobromination in the microreactor is possibly due to its superior heat/mass transfer efficiency compared to that of batch reactor.

Table 3 shows the composition of postreaction solution from the continuous synthesis of *p*-DEB in the two-stage microreactor system, from which a 99.2% yield of *p*-DEB was achieved with a total residence time of approximately 14 s under optimized reaction conditions, corresponding to a throughput of 0.25 kg/h *p*-DEB. The microreactor system not only achieved a much higher *p*-DEB yield than state of the art yield (70%–75%)[1] from semi-batch operations, but shortened the reaction time by three orders of magnitude. Moreover, without restriction on reactant concentrations, the microreactor operation can lead to more concentrated *p*-DEB in the postreaction solution, which is beneficial to the downstream separation.

For production scale-up, issues of large-scale use of Br_2 need to be addressed due to its high volatility, corrosivity, and toxicity. Continuous in situ Br_2 generators consisting of a bromide ion source combined with an oxidant under acidic conditions, as reported by Kappe et al.,[38] can be considered to overcome the drawbacks of large-scale use of Br_2. Alternatively, the Br_2/CCl_4 solution used in the current study could be sealed by a small amount of water as the upper layer to mitigate evaporation of Br_2 during its large-scale use and storage. It should be noted that the use of corrosion resistant materials with high thermal conductivity (Hastelloy, SiC, etc.) for microreactors and their pumping systems is crucial to enable this technology to succeed on large-scale preparations. Typical scale-up strategies for a microreactor based process include numbering up, sizing up and their combinations.[39] Ideally, the scale-up design of microreactor system needs to keep the mixing, residence time (and distribution), and heat transfer identical to its laboratory scale. Given the strong exothermic feature of the reaction and its high temperature sensitivity, numbering up the single unit is recommended as a facile route to increase the throughput of the *p*-DEB production. Sizing up could also be considered to decrease the cost of the reactors, but the unit should be reoptimized through reactor modeling and simulation where effects of back-mixing and radial temperature gradient need to be reevaluated.

4 | CONCLUSION

PAA resins have wide applications due to their outstanding heat resistance, excellent process properties as well as good electrical/optical properties. However, their full commercial development has been impeded by the absence of an efficient synthesis and separation method of their monomer, *p*-DEB. In the current study, we explored a complexation/decomplexation method to purify *p*-DVB from its isomer rich commercial crude and achieved a *p*-DVB purity over 99%. The purified *p*-DVB was then subjected to consecutive bromination and dehydrobromination to produce *p*-DEB without the necessity of downstream isomer separation. Subsequently, reaction pathways and cause of side reactions were revealed through a combined effort of byproduct characterization and DFT calculations, which demonstrates the thermal runaway derived from the exothermic bromine addition (target reaction) would favor aromatic substitution (side reaction) due to much higher E_a of the latter. To address this issue, a microreactor system was developed to enhance heat transfer during the bromination. Owing to the precise temperature control and high mixing efficiency provided by the microreactor system, an unprecedented *p*-DEB yield of 99.2% was achieved under optimal operating conditions with a reaction residence time of only 14 s. Therefore, the efficiency of *p*-DEB production was improved enormously in the microreactor system, given that state of the art yield of *p*-DEB is only 70%–75% after hours of reaction from conventional batch operations. The microreactor system can also generate more concentrated *p*-DEB by overcoming restriction of reactant concentration associated with batch operations, which is beneficial to its downstream separation. To the best of our knowledge, this work demonstrates, for the first time, the use of a microreactor system for efficient and safe production of *p*-DEB, which reveals a new avenue to boost commercial development of PAA resins.

ACKNOWLEDGMENT

This work was supported by the National Natural Science Foundation of China (21991103, 21991104, 22008074, 22008072); Natural Science Foundation of Shanghai (20ZR1415700), China Postdoctoral Science Foundation (2020M671025, 2019TQ0093).

AUTHOR CONTRIBUTIONS

Zhirong Yang: Funding acquisition (equal); investigation (lead); writing – original draft (lead); writing – review and editing (equal). **Yue Yang:** Formal analysis (equal); investigation (equal); software (equal). **Xuefeng Zhang:** Conceptualization (lead); investigation (supporting); validation (lead). **Wei Du:** Investigation (equal); software (equal); validation (equal). **Jing Zhang:** Funding acquisition (lead); supervision (lead); validation (lead); writing – review and editing (lead). **Gang Qian:** Data curation (equal); formal analysis (equal); validation (equal). **Xuezhi Duan:** Data curation (equal); formal analysis (equal); validation (equal). **Xinggui Zhou:** Conceptualization (equal); resources (equal); supervision (equal).

DATA AVAILABILITY STATEMENT

The data that support the findings of this study are available from the corresponding author upon reasonable request.

ORCID

Zhirong Yang https://orcid.org/0000-0003-4417-4814
Jing Zhang https://orcid.org/0000-0002-8213-4314
Gang Qian https://orcid.org/0000-0001-5258-1319
Xuezhi Duan https://orcid.org/0000-0002-5843-5950
Xinggui Zhou https://orcid.org/0000-0002-4736-3672

REFERENCES

1. Carosino LE, Herak DC; Hercules-Incorporated. Synthesis of diethynylbenzene. US patent 4,997,991. 1991.
2. Lin VSY, Radu DR, Han MK, et al. Oxidative polymerization of 1,4-diethynylbenzene into highly conjugated poly(phenylene butadiynylene) within the channels of surface-functionalized mesoporous silica and alumina materials. *J Am Chem Soc*. 2002;124:9040-9041.
3. Kim Y, Kwon S, Yoo D, Rubner MF, Wrighton MS. A novel, bright blue electroluminescent polymer: a diphenylanthracene derivative. *Chem Mater*. 1997;9:2699-2701.
4. Yang QG, Si JH, Wang YG, Ye PX. Phase-modulation effects in self-diffraction. *Phys Rev A*. 1996;54:1702-1708.
5. Zhan XW, Yang MJ, Lei ZQ, et al. Photoluminescence, electroluminescence, nonlinear optical, and humidity sensitive properties of poly(p-diethynylbenzene) prepared with a nickel acetylide catalyst. *Adv Mater*. 2000;12:51-53.
6. Yanovskii LS, Lempert DB, Raznoschikov VV, et al. Prospects for the use of diethynylbenzene as a fuel dispersant for rocket ramjet engines. *Russ Chem B+*. 2019;68:1848-1855.
7. Wu YS, Yu RB, Hu L, Li QQ, Zhu CJ. Thermal stability of cocured blends of vinyl trimethoxysilane and aryl acetylene resins with different posttreatments. *J Appl Polym Sci*. 2014;131:40158.
8. Li QQ, Yu RB, Zhu C, Jiao Z. 60Co γ-rays irradiation modified p-diethynylbenzene as prepolymers to prepare polyarylacetylene with excellent heat resistance. *Polym Degrad Stabil*. 2015;114:81-88.
9. Wang MC, Zhao T. Polyarylacetylene blends with improved processability and high thermal stability. *J Appl Polym Sci*. 2007;105:2939-2946.
10. Njuguna J, Pielichowski K, Desai S. Nanofiller-reinforced polymer nanocomposites. *Polym Adv Technol*. 2008;19:947-959.
11. Sun HJ, Neumann C, Zhang T, et al. Poly(1,4-diethynylbenzene) gradient homojunction with enhanced charge carrier separation for photoelectrochemical water reduction. *Adv Mater*. 2019;31:e1900961.
12. Kim K, Kang T, Kim M, Kim J. Three-dimensional entangled and twisted structures of nitrogen doped poly-(1,4-diethynylbenzene) chain combined with cobalt single atom as a highly efficient bifunctional electrocatalyst. *Appl Catal B Environ*. 2020;275:119107.
13. Safari P, Moggach SA, Low PJ. Mix and (Mis)match: further studies of the electronic structure and mixed-valence characteristics of 1,4-diethynylbenzene-bridged bimetallic complexes. *Dalton Trans*. 2020;49:9835-9848.
14. Li X, Zhang YC, Zhao Y, Zhao HP, Zhang B, Cai T. Xanthene dye-functionalized conjugated porous polymers as robust and reusable photocatalysts for controlled radical polymerization. *Macromolecules*. 2020;53:1550-1556.
15. Shields EP, Weber SG. A pH-stable, crosslinked stationary phase based on the thiol-yne reaction. *J Chromatogr A*. 2019;1598:132-140.
16. Neenan TX, Whitesides GM. Synthesis of high carbon materials from acetylenic precursors. Preparation of aromatic monomers bearing multiple ethynyl groups. *J Org Chem*. 1988;53:2489-2496.
17. Ortaggi G, Sleiter G, D'Ilario L, Bolasco A, Chimenti F. ChemInform abstract: a convenient procedure for the synthesis of bis(ethynyl)benzene derivatives. *ChemInform*. 1989;20:50-51.
18. Watson JM. Synthesis of diethynylbenzenes. *Macromolecules*. 1972;5:331-332.

19. Chimenti F, Bolasco A, Secci D, Chimenti P, Granese A. Synthesis of new diethynylbenzene derivatives. *Synthetic Commun*. 2011;34:2549-2555.
20. Cai LZ, Qiu HX, Wang HT, Yang M, Shen YJ. Synthesis of m/p-diethynylbenzene. *J Chem Eng Chin Univ*. 2008;22:630-633.
21. Allan H. Preparation of *m*- and *p*-diethynylbenzenes. *J Org Chem*. 1960;25:637-638.
22. Yang FH, Hernandez-Maldonado AJ, Yang RT. Selective adsorption of organosulfur compounds from transportation fuels by π-complexation. *Sep Sci Technol*. 2005;39:1717-1732.
23. Tang RY, Tian YY, Wang SJ, Qiao YY, Leng GL. Cu-based π-complexation adsorbent for paraffin/olefin separation in slurry bed. *J Chem Soc Pak*. 2017;39:788-792.
24. Yang RT, Kikkinides ES. New sorbents for olefin/paraffin separations by adsorption via π-complexation. *AIChE J*. 1995;41:509-517.
25. Miklis PC, Ditchfield R, Spencer TA. Carbocation−π interaction: computational study of complexation of methyl cation with benzene and comparisons with related systems. *J Am Chem Soc*. 1998;120:10482-10489.
26. Zhang J, Wu W, Qian G, Zhou XG. Continuous synthesis of methyl ethyl ketone peroxide in a microreaction system with concentrated hydrogen peroxide. *J Hazard Mater*. 2010;181:1024-1030.
27. Cossi M, Rega N, Scalmani G, Barone V. Energies, structures, and electronic properties of molecules in solution with the C-PCM solvation model. *J Comput Chem*. 2003;24(6):669-681.
28. Murdoch JR. What is the rate-limiting step of a multistep reaction? *J Chem Educ*. 1981;58(1):32-36.
29. Nie XW, Janik MJ, Guo XW, Song CS. Shape-selective methylation of 2-methylnaphthalene with methanol over H-ZSM-5 zeolite: a computational study. *J Phy Chem C*. 2012;116(6):4071-4082.
30. Zhang CH, Cao HJ, Wang C, He MX, Zhan WC, Guo YL. Catalytic mechanism and pathways of 1,2-dichloropropane oxidation over $LaMnO_3$ perovskite: an experimental and DFT study. *J Hazard Mater*. 2021;402:123473.
31. Yang CF, Shi Y, He K, et al. Understanding of two-stage continuous microreaction technology for in-situ generation and consecutive conversion of diazomethane. *J Taiwan Inst Chem E*. 2019;98:94-98.
32. Peng XF, Peterson GP, Wang BX. Heat transfer characteristics of water flowing through microchannels. *Exp Heat Transfer*. 1994;7:265-283.
33. Mala GM, Li DQ. Flow characteristics of water in microtubes. *Int J Heat Fluid Flow*. 1999;20:142-148.
34. Koo J, Kleinstreuer C. Liquid flow in microchannels: experimental observations and computational analyses of microfluidics effects. *J Micromech Microeng*. 2013;1(3):568-579.
35. Wu W, Qian G, Zhou XG, Yuan WK. Peroxidization of methyl ethyl ketone in a microchannel reactor. *Chem Eng Sci*. 2007;62:5127-5132.
36. Duan XZ, Huang ZK, Qian G, et al. Unprecedented yield of methyl-esterification with in-situ generated diazomethane in a microchannel reactor with methanol as solvent. *Chem Eng Sci*. 2020;213:115397.
37. Cantillo D, Kappe CO. Halogenation of organic compounds using continuous flow and microreactor technology. *React Chem Eng*. 2017;2:7-19.
38. Steiner A, Roth PMC, Strauss FJ, et al. Multikilogram per hour continuous photochemical bvenzylic brominations applying a smart dimensioning scale-up strategy. *Org Process Res Dev*. 2020;24:2208-2216.
39. Lv HC, Yang ZR, Zhang J, et al. Liquid flow and mass transfer behaviors in a butterfly-shaped microreactor. *Micromachines*. 2021;12:883.

SUPPORTING INFORMATION

Additional supporting information may be found in the online version of the article at the publisher's website.

How to cite this article: Yang Z, Yang Y, Zhang X, et al. High-yield production of *p*-diethynylbenzene through consecutive bromination/dehydrobromination in a microreactor system. *AIChE J*. 2022;68(2):e17498. doi:10.1002/aic.17498